Fracture 1977, Volume 1, ICF4, Waterloo, Canada, June 19 - 24, 1977

MECHANISM OF EMBRITTLEMENT AND BRITTLE FRACTURE IN LIQUID METAL ENVIRONMENTS

M. H. Kamdar*

ABSTRACT

Polycrystals and single crystals of normally ductile metals fail in a catastrophic brittle manner when exposed to certain surface active liquid metal environments. The fracture mode changes from ductile to intergranular or transgranular mode or both. In some instnaces, propagation of cracks in liquid metal environments occur at speeds of order 100 cm/sec. Such effects are generally recognized as the phenomena of "Liquid Metal Embrittlement". Liquid metal embrittlement is presently considered to result from liquid metal "adsorption-induced reduction in cohesion" of atomic bonds at regions of high stress concentrations in a solid, such as at the tips of cracks or at the sites of crack nucleation. The prerequisites for embrittlement are the same as those for brittle fracture and liquid metal embrittlement is considered a special case of brittle fracture rather than a diffusion or a corrosion type of phenomena. This paper presents some theoretical considerations (1) concerning the "reduced-cohesion" mechanism of embrittlement and (2) embrittlement to be a special case of brittle fracture. Experimental results utilizing ideal embrittlement systems in support of the mechanism and also in support of various brittle fracture criteria are presented and discussed.

INTRODUCTION

When an oxide-free solid metal is coated with a thin film of a liquid metal only a few microns in thickness and then immediately deformed in tension, its yield and flow behavior are not significantly affected. Its fracture behavior, however, can be markedly different from that observed in air. In many instances a reduction in fracture stress or strain results, Figure 1, the magnitude of which is dependent on various chemical and mechanical parameters of the solid metal-liquid metal system. Under certain experimental conditions, embrittlement can be quite dramatic, specimens stressed above some critical value appear to fail "instantly" on wetting or contacting with an appropriate liquid metal. The polycrystalline metals usually fail by an intergranular mode in liquid metal environments. However, it is also possible to cleave monocrystals of otherwise ductile metals such as cadmium in certain liquid metal environments (see Table 1 and Figure 2). Also, brittle crack propagation rates of order 50-500 cm/per second have been reported for ductile aluminum alloys in liquid mercury environments. Such effects occur only in specific solid metal-liquid metal couples and belong to the class of environment-sensitive fracture phenomena known as liquid-metal embrittlement.

*Materials Engineering Division, Benet Weapons Laboratory, Watervliet Arsenal, Watervliet, New York, U.S.A.

Embrittlement by liquid metals can also occur in the absence of stress by intergranular penetration of liquid metal into the solid metal or in the presence of stress, by corrosion or by diffusion controlled processes. Such time and temperature dependent processes are not considered responsible for the occurrence of liquid metal embrittlement [1]. The tensile fracture stress of the solid metal coated with the liquid metal does not depend upon the time of exposure to the embrittling liquid metal prior to testing [1], or upon whether the liquid metal is pure or presaturated with the solid metal. Severe embrittlement of the solid metal occurs near the freezing temperatures of the liquid metal environments [4]. The presence of a grain boundary is not a prerequisite for the occurrence of embrittlement, since monocrystals of ductile metals such as zinc [5] and cadmium [5,6] are known to fracture by cleavage in liquid gallium and other liquid metal environments. Accordingly, this paper will not be concerned with embrittlement effects by liquid metals which are caused by corrosion or diffusion controlled processes, it will instead concentrate on those examples of liquid metal embrittlement of a solid metal presently considered to result from liquid metal adsorption induced brittle fracture.

It is considered that embrittlement results from a liquid metal chemisorption-induced reduction in the strength of atomic bonds at the regions of stress concentrations in a solid metal such as at the tip of a crack [4,7], or at the head of a dislocation pile up near an obstacle in the surface of the solid [8]. Embrittlement in liquid metal environments may be considered as a special case of brittle fracture, and that the effects of mechanical, metallurgical, physical and chemical factors on embrittlement may be explained rationally in terms of the principles of brittle fracture [8]. The purpose of this paper is to document advances made in the understanding of the phenomena of liquid metal embrittlement and also to discuss these by considering embrittlement as a special case of brittle fracture and in terms of the prevalent "adsorption-induced reduction in cohesion" mechanism of embrittlement [4,7,10]. For more detailed account of this phenomena the reader is referred to the recent major review by Kamdar [1].

MECHANISMS OF LIQUID METAL EMBRITTLEMENT

2.1 Reduction in surface energy model

Several workers have porposed that liquid metal embrittlement is associated with a reduction in the surface free energy of the solid metal by the adsorbing liquid metal species [2,5,9]. This is obvious since embrittlement effects must originate at the solid-liquid metal interface and hence energy considerations of the interface must be important. Nevertheless, such a thermodynamic approach is not particularly informative because it does not provide insights into the mechanism of embrittlement on an atomic or electronic scale.

2.2 Adsorption-induced reduction in cohesion model

In view of the limitation of the above approach, it is usggested that one should focus attention at the crack tip and consider the effects of the adsorption of the liquid metal species at or in the vicinity of the tip before attempting to understand the mechanism of the embrittlement process [1,10]. In this regard, it has been suggested that embrittlement is associated with a localized reduction in the strength of atomic bonds at the crack tip or at the surface of the solid metal by certain chemisorbed species [1,4]. With this possibility in mind, consider the crack shown in Figure 3. Crack propagation will occur by repeatedly breaking of bonds

of the type A-A_o, A-A_1, etc. Such bonds might be expected to have potential energy-separation distance curves of the form U(a) indicated in Figure 4, a_o being the equilibrium distance between atoms across the fracture plane. The resulting stress, σ, between atoms A and A_o as they are separated, varies as (dU/da) from $\sigma = 0$ at $a = a_o$, to a maximum value of $\sigma = \sigma_m$ at the point of inflection U_1 of the curve U(a). It follows that a tensile stress of magnitude σ_m acting at the crack tip would cause the bond A-A_o to break. Assuming that the actual σ(a) curve can be approximated by one-half of a sine curve, and that its half wavelength, λ, represents the effective range of the interatomic forces, it can be shown that [11]

$$\sigma_m = (E\lambda/\pi a_o) \quad . \tag{1}$$

If the work done in breaking A-A_o bonds is then equated to the surface free energy of the subsequently created fracture surfaces, γ, it can also be shown that [11]

$$\sigma_m = (E\gamma/a_o)^{1/2} . \tag{2}$$

Next assume that the liquid metal atom B, (a vapor phase or an elemental gas such as atomic or molecular hydrogen may also provide the embrittling atom B) at the crack tip reduces the strength of the bond A-A_o. The chemisorption reaction presumably involved in such a process may occur spontaneously (i.e. in time less than that required in a mechanical test), or only after atoms A and A_o have been strained to some critical separation distance, a_c. In any event, as a result of the electronic rearrangement involved in this process the bond A-A_o becomes inherently weaker, and thus the form and displacement of its potential energy-separation curve may now be considered similar to $U(a)_B$, Figure 4. As the applied stress is increased, the stress acting on bond A-A_o eventually exceeds its now reduced breaking stress, $\sigma_{m(B)}$, the bond breaks, the crack propagates to Y; Figure 3, and atom B becomes stably chemisorbed on the freshly created surface. This procedure is then repeated until the specimen fails. The cracking process is limited by the arrival of liquid metal atoms at the crack tip and it is assumed that liquid is able to keep up with the propagating crack tip.

According to this hypothesis, crack initiation at the surface will also be facilitated by the adsorption of liquid metal B atoms. Moreover, if chemisorption is strain-activated, it will occur preferentially at sites of stress concentration, such as in the vicinity of piled-up groups of dislocations at high angle grain boundaries.

Theoretical studies of the interactions between single adsorbed atoms and metal surfaces are now being undertaken. Unfortunately, however, these studies are not yet sufficiently advanced to provide predictions of specific embrittlement behavior. The same problem arises when one looks for experimental techniques that are capable of detecting any adsorption-induced variation in electron distribution in the surface bonds which may lead to weakening without applying a stress.

An alternative approach is first to determine the true fracture surface energy for the cleavage plane of a particular solid metal, γ, which is directly related to $\sigma(\sigma = \sigma_m)$ in equation (2), and then show that γ is reduced in the presence of an active liquid metal. Such an analysis has been made by Westwood and Kamdar [4].

$$\sigma_p \text{ (blunted crack)} = (E\rho\gamma/4c)^{1/2} \quad . \tag{3}$$

Here σ_p is the stress to propagate a crack, the energy ϕ_p involved in propagating a blunted crack is simply $(\rho\gamma)$, where ρ is a dimensionless, variable ratio of the radius at the crack tip R_1 and a_o the atomic spacing (R_1/a_o) dependent upon the amount of plastic relaxation at the crack tip, and therefore upon temperature, propagation rate, yield stress, metallurgical composition and structure, etc.

Note that this analysis suggests that the crack propagation energy, ϕ_p, is related directly to the surface free energy, γ, and should not be thought of as the *sum* of the surface free energy *plus* a plastic relaxation energy, p. It will be appreciated that if ϕ_p is equated to $(\gamma + p)$, and $p > \gamma$ - as is ordinarily the case for ductile metals - it is difficult to see how the magnitude of ϕ_p could be significantly affected by the testing environment.

It should also be noted from Figure 3, that because of the presence of embrittling liquid-metal atom B at or near the crack tip, it is only necessary that the strength of the bond A-A_o be affected. In other words, the embrittling action of B is independent of the radius of the crack tip. This possibility leads to the suggestion that it might be useful to define a coefficient of embrittlement for crack propagation, η_p, relating the energy adsorbed in breaking bonds at the crack tip in the presence and absence of an embrittling phase. A convenient definition is

$$\eta_p = \phi_{PA(B)}/\phi_{PA} = \gamma_{A(B)}/\gamma_A, \quad \rho = 1. \tag{4}$$

The total energy involved in the propagation of a crack in a metal, ϕ_p, can then be written as

$$\phi_p = (\eta\rho\gamma) \tag{5}$$

where η and ρ are simple and independent ratios, η being an environmental variable, and ρ a plastic relaxation variable.

Equations (4) and (5) suggest that embrittlement may occur by "liquid-metal adsorption-induced reduction in cohesion mechanism" if the coefficient of embrittlement, η_p, determined for both atomically sharp and plastically blunted cracks is less than unity, i.e. γ A(B) $< \gamma$(A), or ϕ_p A(B) $< \phi_p$(A).

A double cantilever cleavage technique has been used by Gilman [12] and others [4,13] to introduce cleavage cracks in crystals and to determine the energy to propagate cracks on the cleavage plane of ionic, covalent, and metallic monocrystals. For these crystals, the experimentally determined values of ϕ_p are in good agreement with the values of the cleavage surface energies derived from theoretical considerations [14]. This experimental technique therefore provides a possible method for determining cleavage surface energies of metal single crystals when the liquid metal environment is present at the crack tip. Accordingly, Westwood and Kamdar have used this technique to examine the validity of the above approach by studying cleavage crack propagation on the basal plane of zinc monocrystals in liquid mercury, liquid gallium and inert environments.

2.3 Crack propagation in the zinc-mercury and zinc-gallium system

2.3.1 *Determination of cleavage fracture energies*

Westwood and Kamdar [4] used the double cantilever cleavage technique to determine values of ϕ_p for zinc from liquid nitrogen temperature to 60°C, and for the zinc-liquid mercury embrittlement couple from the melting point of mercury, -39°C, to 60°C. A diagram of the type of specimens used is included in the inset in Figure 5. Following Gilman [12] the cleavage fracture energy, ϕ_p, was computed from the relationship

$$\phi_p = (6F^2L_o^2/Ew^2t^3) \tag{6}$$

where F is the load to propagate a pre-existing crack of length L_o (introduced at -196°C), and w and t are the specimen dimensions designated in the figure. The results are presented in Figure 5. It can be seen that the value of ϕ_p for zinc, 90 $\pm$ 10 ergs/cm^2, is essentially independent of temperature. This value is in fair agreement with that of ~185 ergs/cm^2 for the cleavage energy of the basal plane in zinc derived by Gilman [14] from theroetical considerations. This value is therefore regarded as the true fracture surface energy for cleavage on the basal plane of zinc, i.e. γ(Zn). When liquid mercury was present at the crack tip, however, ϕ_p was reduced to 53 $\pm$ 8 ergs/cm^2. The coefficient of embrittlement of zinc mercury couple, η_p(Zn-Hg) = ϕ_p(Zn-Hg)/ϕ_p(Zn), ρ = 1 is 0.61 $\pm$ 0.12. It will be shown later that this value is identical with that for the energy to initiate a crack in zinc in the presence of liquid mercury (50 $\pm$ 3 ergs/cm^2) as is to be expected since both crack initiation and propagation occur in the basal plane and involve the breaking of zinc-zinc bonds across the fracture plane.

Similar experiments were also performed using liquid gallium as the embrittling liquid metal for zinc. In this case, ϕ_p(Zn-Ga) was 42 $\pm$ 13 ergs/cm^2 and η_p = 0.48 $\pm$ 0.17, indicating that liquid gallium is more embrittling then is liquid mercury for zinc. Several tests were made in which liquid mercury presaturated with zinc was used as the embrittling environment. Again ϕ_p was ~53 ergs/cm^2, thus providing support for the view that liquid metal embrittlement does not involve a simple dissolution effect [4].

It may be concluded from this work that the values of ϕ_p observed in the presence of liquid mercury or gallium, which are less than γ for the basal plane of zinc, provide support for the reduction-in-bond-strength model for liquid metal embrittlement. The theoretical estimates of the reduction in cohesion of zinc in liquid mercury and gallium environments are not available at the present time. The variation in the values of η_p observed in liquid mercury and gallium suggest, nevertheless, that the severity of embrittlement is probably related to the chemical nature of these species.

2.3.2 *Effects of plastic deformation and environment on ϕ_p*

In studies similar to those described above, Westwood and Kamdar [4] also investigated the effects of plastic blunting of the crack tip on crack propagation and determined ϕ_p and η_p for zinc in liquid mercury and inert environments. Following double-propagation technique was adopted for most of the experiments. A long crack was initiated in zinc monocrystals at room temperature in air, and the load to propagate this crack a small distance was determined. Following propagation of the crack the specimen was unloaded and a drop of mercury introduced in the crack. The specimen

was reloaded and fracture was completed. The values of ϕ_p(Zn, 298°K) and ϕ_p(Zn-Hg, 298°K) were computed using equation (6). The experimental data are presented in Figure 6. It was observed that $\phi_p(\text{Zn-Hg})/\phi_p(\text{Zn}) = 0.61 \pm .07$, and a line of slope 0.61 drawn in Figure 6 illustrates a good fit to the data. Thus, for plastically blunted cracks η_p(Zn-Hg) at 298°K is 0.61 and is the same as that determined for atomically sharp cracks. The results provide support for the validity of equation (4) when $\rho > 1$ and in addition indicates that in the case of plastically blunted cracks, embrittlement may also be considered to occur by the adsorption-induced reduction in cohesion mechanism. Thus, due to the reduction in cohesion of atomic bonds at the crack tip, a lower stress concentration at the tip is required to propagate a blunted crack in a liquid metal than that in an inert environment. Similar reasoning can readily be applied to most embrittlement couples where plastic flow invariably precedes embrittlement.

BRITTLE FRACTURE IN LIQUID METAL ENVIRONMENTS

3.1 A criterion for ductile-brittle fracture and embrittlement

At the present time, it is considered that the phenomena of liquid metal embrittlement and effects of various factors (mechanical, metallurgical, physical and chemical) on embrittlement can be interpreted rationally by considering the interaction of the embrittling species at or in the vicinity of the crack tip. We have discussed embrittlement as a consequence of the chemisorption induced reduction in cohesion, actually reduction in the tensile stress at a crack tip. This assumption together with consideration of the effects of the short range nature of the interaction between the adsorbed species and metallic surfaces on shear strength (actually plastic deformation or stress to move or multiply dislocations) at the crack tip, suggests that liquid metal embrittlement may be considered a special case of a general criterion for predicting the ductile or brittle behavior of solids presented earlier by Gilman [11] and discussed in detail recently by Kelly et al [15]. The argument presented by the latter is essentially as follows: An equilibrium crack in a solid subjected to an increasing force F, Figure 7, will propagate in a fully brittle manner by cleavage, (it is suggested here that the term "cleavage" may be used in connection with brittle crack propagation by either transcrystalline or intercrystalline paths), if the ratio of the largest tensile fracture stress, σ, in the vicinity of the crack tip to the largest shear stress, τ, on the most favorably oriented slip plane S-P near the tip is greater than the ratio of the ideal cleavage stress, σ_{max} to the ideal shear stress τ_{max}. If the converse is the case, then the crack propagation will be accompanied with some plastic flow. As a rough approximation for metals, if the ratio σ_{max}/τ_{max} is ≤ 10, then failure will be predominantly by cleavage. If σ_{max}/τ_{max} is ≥ 10 failure will be predominantly by shear. The appropriate values of these ratios are determined by the type of bonding in the solid (i.e. ionic, metallic, etc.), by its crystal structure and the Poisson's ratio, ν. The values of these ratios for some typical solid metals which are embrittled by liquid metals are given in Table 2.

Consider now the effect of a surface-active liquid metal atom B at the crack tip of A-A_o in Figure 7. As a consequence of the chemisorption of this atom, and for reasons discussed earlier, it is suggested that some variation in the strength of the bond between the atoms A and A_o will result, and hence the magnitude of σ_{max} will be changed. On the other hand, because of free electron screening effects in a metal caused by the presence of high concentration of mobile conduction electrons, the effects of such a chemisorbed liquid-metal atom will not be felt at depths greater than a

few atom diameters from the crack tip, S. Thus, the chemisorbed atom will be unlikely to influence the strength of bonds across the slip plane S-P for a distance from S sufficient to significantly affect the ease of dislocation motion in the vicinity of the crack tip. As far as plastic deformation in the vicinity of the crack tip is concerned, it follows that the magnitude of τ_{max} should be considered unaffected by the presence of atom B.

If the adsorption of liquid-metal atom B leads to a reduction in σ_{max} while τ_{max} is unaffected, then the ratio σ_{max}/τ_{max} will be decreased. This effect will be manifested is an increased tendency to cleavage, i.e., as some degree of liquid-metal embrittlement, (providing there is an adequate supply of liquid metal atoms, and their diffusion rate is sufficient to allow them to keep up with the propagating crack tip), the severity of which will be related to the magnitude of the reduction of σ. The above reasoning may be used to explain liquid metal embrittlement of normally ductile face centered cubic metals such as copper, silver, gold and aluminum. For most embrittlement couples, the yield stress and stress-strain or flow behavior of the solid metal tested in air or in an inert environment remains unaffected when tested in an embrittling liquid metal environment, [1,2,6,8] Figure 1. This indicates that as postulated τ_{max} and τ are not affected by the adsorption of the liquid metal on the surface of the solid. However, experimental determination of the cleavage fracture energy of zinc, (Zn) in an inert and liquid mercury or gallium environment indicate that in liquid metal environments σ_{max} may decrease by some 40 to 50%. Such measurements are difficult to make for most metals, because they are ductile and difficult to cleave. Nevertheless, let us assume that for these metals, liquid metal adsorption may reduce σ_{max} by about 40 to 50%. Since τ_{max} is not affected, the value of the ratio σ_{max}/τ_{max} for Cu, Ag, and Au in liquid metal environments will be about half of the values listed in Table 2 for these metals in inert environments. Note that the decreased values are about the same as the value of the ratio, σ/τ given in the same Table 2. Thus, in accord with Kelly et al's criterion, in liquid metal environments one would predict a transition from ductile to brittle behavior for these metals. Similar reasoning may be used in a qualitative manner to explain the transition from pure shear type failure in inert environment at liquid helium temperature to brittle cleavage in liquid metal environments at elevated temperatures observed in aluminum and cadmium monocrystals [16,6]. Aluminum monocrystals failed by (001) type cleavage in liquid gallium at 30°C [16], where as cadmium monocrystals failed by basal cleavage in liquid gallium [1] and in mercury-indium solutions at 30°C, [6], Figure 2.

From the foregoing, it may be suggested that while considering the phenomena of liquid metal embrittlement, it is a convenient first approximation to think of σ as the environment-sensitive parameter, and τ as the metallurgical structure-sensitive parameter. These parameters are not always independent, alloying can affect both σ and τ, but where appropriate, this simple approach will be adopted in this paper.

The severity of embrittlement observed is also dependent upon the metallurgical-structure dependent factors which determine τ. Thus, embrittlement observed in a solid in a pure liquid metal depends also upon factors that affect the solid, e.g. alloying additions, cold work, temperature, grain size, the microstructure and the mechanical variables. The effects of these factors on embrittlement may be interpreted by considering the ease or the difficulty with which relaxation of stress concentrations via plastic deformation may occur at the tip of the crack during crack nucleation or crack propagation [1]. The effects of these factors on embrittlement therefore are related to the magnitude of the structure-sensitive

parameter, τ. Increase in τ will decrease the ratio, σ/τ, thus causing an increase in the susceptibility to embrittlement conversely a decrease in τ (e.g. by an increase in temperature or grain size and decrease in strain rate) may increase the ratio, σ/τ, and thus causing a decrease in the susceptibility to embrittlement.

In addition to the above considerations, there should also be a sufficient supply of the active liquid to ensure adsorption at a crack nucleation site, and subsequently at the propagating crack tip. It is possible, however, that if fracture in a liquid metal environment is nucleation controlled then once initiated the crack may propagate to failure regardless of the presence of the liquid at the tip as for example was noted in the case of Fe-3% Si monocrystals tested in Hg-In solution [1]. On the other hand, if fracture in a liquid metal environment is propagation controlled, a crack may not nucleate in a liquid metal environment in a smooth specimen, (i.e. embrittlement will not be observed). But in a notched specimen, a sharp crack will propagate to failure in the presence of the liquid at the tip, i.e. embrittlement will be noted if a stress raiser is present. Such a behavior was observed in Iron-Nickel alloys tested in a liquid mercury environment [17].

It is realized that certain factors such as alloying, temperature, etc., may vary the magnitude of both σ and τ, and that various mechanical, physical and chemical factors not only operate simultaneously but are interrelated. Nevertheless, the above simple approach appears to provide a rational interpretation for embrittlement effects that have been observed when one variable was investigated in a simple well characterized system. Some of the important factors on the severity of liquid metal embrittlement are considered in more detail in a major review paper by Kamdar [1], utilizing examples of well characterized simple embrittlement couples taken from the extensive but unfortunately not always reliable literature on liquid metal embrittlement. The above considerations and available experimental evidence do in fact suggest that embrittlement in a liquid metal environment may be considered a special case of the general criterion which Kelly et al [15] have developed for predicting the ductile-brittle behavior of solids.

Concerning brittle fracture, however, Kamdar and Westwood [8] have used liquid metal environments to demonstrate that the prerequisites for liquid metal adsorption-induced brittle fracture are the same as that for brittle fracture in inert environments and that such environments may be used instead of low temperatures and inert environments to test the validity of several fracture criteria. The objective of such investigations was to show that adsorption induced embrittlement is truly a special case of brittle fracture and is not a corrosion or dissolution dependent phenomena. With this in mind, we will present and discuss the extensive investigations by Kamdar and Westwood [8] on brittle fracture in the zinc in liquid mercury environments.

3.2 Prerequisites for embrittlement

Certain prerequisites must be fulfilled before fracture can initiate in a metal in liquid metal environment. For a ductile, unprecracked metal specimen these are (i) an applied tensile stress, (ii) some measure of plastic deformation, and (iii) the existence in the specimen of some stable obstacle to dislocation motion, capable of serving as a stress concentrator; this obstacle can be either pre-existing (e.g. a grain boundary) or created during deformation (e.g. a kink band). In addition, there should also be

a sufficient supply of the active liquid metal to ensure adsorption at this obstacle, and subsequently at the propagating crack tip. These prerequisites are the same as those for brittle fracture at low temperature. The experimental evidence for the prerequisites for liquid metal is presented elsewhere [8,10].

3.3 Criteria for crack initiation

Several criteria have been proposed for crack initiation in solids which slip and cleave on the same plane, and also contain a suitable obstacle to slip. Such criteria, of course, apply to brittle failure in general. However, by optimizing the conditions for brittle behavior, deformation in active liquid metal environments has proved to be a very convenient method of examining both their qualitative and quantitative validity. The various fracture criteria by Gilman [18], Likhtman and Shchukin [9], Stroh [19], Bullough [20], and Kamdar and Westwood [8,12] have been described elsewhere and are then compared with experimental data obtained from studies on the zinc-liquid mercury system [8].

3.4 Crack initiation in pure zinc

Studies of the fracture behavior of asymmetric bicrystals of zinc in liquid mercury at room temperature have provided a convenient means of evaluating the above criteria [8]. The boundary in such crystals (see insert in Figure 8) provides a strong barrier to the emergence of edge dislocations from one of the component crystals, and failure occurs after only 0.5-4% strain. Tensile experiments were performed with two types of asymmetric zinc bicrystals: Type I was grown by electron beam welding two monocrystals together (D_o, the width constant). Type II was grown by seeding (D_o not constant). Both types were 5mm x 10mm in section and 7-9 cm in length, and were amalgamated over the center part of the gauge section only. On testing, cleavage cracks were initiated at the grain boundary, and these propagated completely through the crystals of orientation such as B in Figure 8.

Experimental data points presented in Figures 8 and 9 are from crystals of Type I. The solid curves drawn in Figure 8 correspond to values of σ_{NF} and τ_F derived from various fracture criteria. It can be seen that the theoretical values of τ_F and σ_{NF} calculated from various fracture criteria are in good agreement with experimentally determined values, Figure 8. Figure 9 presents the data again in order to compare it with the Stroh (S) [19], Bullough (B) [20], and Smith-Barnby's (S-B) [22], theoretical estimates of τ_F and σ_{NF}.

Bullough's estimates are in fair agreement with the experimentally determined values except for crystals having $\chi_o > \sim 70°$. However, neither Stroh's nor that of Smith and Barnby's analysis are in accord with the data.

For bicrystals of Type II, grown by seeding, D_o was not constant from specimen to specimen. Accordingly, the test data were examined in terms of the Kamdar-Westwood criteria,

$$\sigma_{NF}\ (\tau_F - \tau_C)\ L_F = 4\phi_I [EG/1-\nu]^{1/2} \qquad (7)$$

where ϕ_I should be independent of the orientation of the bicrystal. (Here τ_C is critical resolved shear stress, L_F is slip plane or pile up length, E and G are Young's and shear modulus, and ν, the Poissons ratio, and

ϕ_I, fracture initiation energy). The data are shown in Figure 13. It is seen that ϕ_I was constant over the range of orientations for which slip might be expected to occur predominantly on the basal plane, and failure by a Bullough-Gilman-Rozhanskii type mechanism. Since ϕ_I was independent of orientation, the cleavage fracture surface energy for the basal plane of zinc in the presence of liquid mercury was calculated from the fracture criterion to be 53 $\pm$ 3 ergs/cm^2. The test data for zinc and it's alloys are given in Table 3.

3.5 The coefficient of embrittlement for crack initiation in Zn-Hg System

In Section 2.2, a coefficient of embrittlement for crack propagation η_p was defined as the ratio $\phi_{p,A(B)}/\phi_{p(A)} = \gamma_{A(B)}/\gamma_A$, ($\rho$ = 1). For zinc-mercury embrittlement couple, $\eta_p = \phi_p$ (Zn-Hg, 298°K)/ϕ_p (Zn, 77°K or 298°K) = γ(Zn-Hg, 298°K)/γ (Zn, 77°K) was 0.61 $\pm$ 0.12. This value which is less than unity was taken to indicate that crack propagation in zinc on the basal plane occurs in accord with the adsorption induced reduction in cohesion mechanism. Since crack nucleation and propagation both occur in the same plane (0001) over the temperature 77°K to 298°K, above observation and a consideration of the mechanism of crack nucleation in the presence and in the absence of an adsorption active liquid metal atoms at or near the obstacle suggested that a coefficient of embrittlement for crack initiation, η_I for a zinc-mercury embrittlement couple may also be defined as the ratio of the energy to break atomic bonds across the fracture plane to initiate a cleavage crack in liquid mercury environments, ϕ_I (Zn-Hg, 298°K) to that in the absence of mercury in an inert environment (e.g. liquid nitrogen) at low temperatures, ϕ_I(Zn, 77°K) [23]. Thus, $\eta_I = \phi_I$ (Zn-Hg, 298°K)/ϕ_I(Zn, 77°K). If crack initiation in liquid mercury and in inert environments at 77°K occurs in a truly brittle manner such that plastic relaxation processes during crack nucleation are minimized; then η_I should be equivalent to the value of the ratio of the cleavage surface energies, γ(Zn-Hg, 298°K)/γ(Zn, 77°K). In this case, η_I would be less than unity. Crack nucleation in zinc in liquid mercury therefore may be considered to occur in accord with the "adsorption-induced reduction in cohesion" mechanism of liquid metal embrittlement. Also, $\eta_I \simeq \eta_p$, since cleavage in zinc is known to initiate and propagate in the same basal (0001) plane [8]. It is generally agreed that fracture in liquid metal environments initiates in most cases by the adsorption-induced reduction in cohesion mechanism [4,7] (Section 2.2 and 2.3). However, no quantitative evidence is yet available in support of the possibility that fracture in these environments may be initiation controlled. Recently, Kamdar [23] has made a quantitative evaluation of the coefficient of embrittlement for crack initiation, η_I, in a zinc-mercury couple by determining reliable values of ϕ_I(Zn, 77°K), the fracture initiation energies of zinc in an inert environment at 77°K and ϕ_I(Zn-Hg, 298°K). Since fracture nucleation in zinc in liquid mercury and in an inert environment at 77°K occurs by basal cleavage and presumably by the same Bullough-Gilman-Rozhanskii-mechanism, it is appropriate to use Kamdar-Westwood fracture criterion for zinc at 77°K. Accordingly, the tensile cleavage fracture data of Deruyetter and Greenough [24] and Shchukin and Likhtman [25] for zinc monocrystals and of Kamdar [26] for asymmetric bicrystals of various orientations, χ_o (where χ_o is the angle between the tensile axis and (0001) cleavage plane at fracture) and different diameters in conjunction with the fracture criterion were used to derive reliable values of ϕ_I(Zn, 77°K) and provide support for the validity of the fracture criterion of Kamdar and Westwood.

In agreement with the prediction form the fracture criterion, it is seen that ϕ_I does not vary significantly with χ_o or a sixfold change in crystal

diameter, Figure 10, the Fracture data is represented by a Petch type fracture stress-grain size relationship, Figure 11, (note that similar relationship was also observed for zinc in mercury environments, Figure 12) and that ϕ_I(Zn, 77°K) = 100 $\pm$ 20 ergs/cm^2, Figure 11, ϕ_I(Zn-Hg) 298°K was ~48 ergs/cm^2, Figure 13. This value is about the same as the (~53 ergs /cm^2) determined earlier in Section 2.5. The value of η_I, the ratio ϕ_I(Zn-Hg) 298°K/ϕ_I(Zn, 77°K) is ~0.50 in agreement with that of 0.61 $\pm$ 0.12 for η_p, the coefficient of embrittlement determined by Westwood and Kamdar [4], (Section 2.2.1). Thus $\eta_I \simeq \eta_p$.

The values ~48 ergs/cm^2 derived for ϕ_I(Zn-Hg, 298°K) and ~100 ergs/cm^2 for ϕ_I(Zn, 77°K) are in good agreement with those of ~53 and 90 ergs/cm^2 for ϕ_p(Zn, 77°K), respectively, determined by Westwood and Kamdar [4], using the double cantilever cleavage technique. The value of ~100 ergs/cm^2 computed for ϕ_I(Zn, 77°K) and ϕ_p(zn, 77°K) is in fair agreement with that of ~185 ergs/cm^2 for γ(Zn), the cleavage surface energy of (0001) plane in Zinc derived by Gilman [12,14] from theoretical considerations. Therefore, both ϕ_I(Zn, 77°K) and ϕ_p(Zn, 77°K) are considered equivalent to γ(Zn, 77°K), the cleavage surface energy of the basal plane in zinc in inert environments at 77°K [26]. This suggests that crack initiation in zinc in liquid nitrogen environment (i.e. at 77°K) occurs at energies which are equivalent to that required to break atomic bonds across the fracture plane, and that only a small amount of energy is absorbed by plastic deformation processes which cause relaxation of stress concentrations at a barrier during crack initiation. The significant observations, however, are that ϕ_I(Zn-Hg, 298°K < ϕ_I(Zn, 77°K) $\simeq$ γ(Zn, 77°K) and the ratio of these energies, η_I is ~0.50. Now, γ(Zn, 77°K) = 90 $\pm$ 10 ergs/cm^2 is about the same as γ(Zn, 298°K) = 87 + 5 ergs/cm^2, Figure 5, γ(Zn) does not vary significantly with the temperature in the range 77°K to 298°K. Therefore, the energy to break bonds across the fracture plane in liquid mercury environments at 298°K is less than the cohesive strength of atomic bonds in an inert environment at 77°K and 298°K [23]. This suggests that adsorption of mercury atoms at the grain boundary in zinc or at the sites of high stress concentrations near a barrier causes reduction in cohesion of atomic bonds across the fracture plane, thereby facilitating crack nucleation in zinc in liquid mercury environments. Therefore, crack initiation in a zinc-mercury couple can be considered to occur by the "adsorption-induced reduction in cohesion" mechanism.

The result, ϕ_I(Zn, 77°K) = ϕ_p(Zn, 77°K) ~ γ(Zn, 77°K), is in good agreement with the condition for nucleation controlled fracture, namely $\phi_I = \phi_p = \gamma$, derived by Stroh [27] and Smith [28] from theoretical considerations. Thus, fracture in zinc in an inert environment at 77°K is shown to be nucleation controlled [26]. Theoretical estimates of γ(Zn-Hg, 298°K) are not available. Nevertheless, since ϕ_I(Zn-Hg, 298°K) ~ ϕ_p(Zn-Hg, 298°K) and $\eta_I \simeq \eta_p$, it is suggested that fracture in zinc in mercury environments may be considered to be nucleation controlled.

Extensive investigations with the model embrittlement couple, zinc and its alloys in liquid mercury environments and at low temperatures in an inert environment discussed in this section provide convincing support for the ideas that liquid metal embrittlement is a special case of brittle fracture and that the embrittlement process occurs by the "adsorption-induced reduction in cohesion" mechanism [23].

REFERENCES

1. KAMDAR, M. H., Embrittlement by Liquid Metals, Prog. Mat. Sci., 15, 1973, 289.
2. ROSTOKER, W., McCAUGHEY, J. M. and MARKUS, M., Embrittlement by Liquid Metals, New York, Reinhold, 1960.
3. STOLOFF, N. S., Liquid Metal Embrittlement, Surface and Interface, II 14, Sagamore Army Mat. Res. Conf., Ed. J. Burke, J., Reed, N., Weiss, W., 1968, 159.
4. WESTWOOD, A. R. C. and KAMDAR, M. H., Phil. Mag., 8, 1963, 787.
5. LIKHTMAN, V. I., SHCHUKIN, E. D. and REBINDER, P. A., Physico-Chemical Mechanics of Metals, Acad. Sci. of USSR, Moscow, 1962.
6. KAMDAR, M. H., Phys. Stat. Solids, 4, 1971, 225.
7. STOLOFF, N. S. and JOHNSON, T. L., Acta. Met., 11, 1963, 251.
8. KAMDAR, M. H. and WESTWOOD, A. R. C., Environment Sensitive Mechanical Behavior, Ed. Westwood, A. R. C. and Stoloff, N. S., Gordon and Breach, New York, 1966, 581.
9. LIKHTMAN, V. I. and SHCHUKIN, E. D., Soviet Physics - Uspekhi, 1, 1958, 91.
10. WESTWOOD, A. R. C., PREECE, C. M. and KAMDAR, M. H., Fracture, Ed. H. Liebowitz, Academic Press, New York, 3, 1971, 589.
11. GILMAN, J. J., Plasticity, Pergamon, New York, 1960, 43.
12. GILMAN, J. J., J. Appl. Phys., 31, 1960, 2208.
13. GOVILA, R. K. and KAMDAR, M. H., Met. Trans., 2, 1970, 1011.
14. GILMAN, J. J., Fracture, Ed. Averbach, B. L., Felback, D. K., Hahn, G. T., and Thomas, D. C., John Wiley and Sons, New York, 1959.
15. KELLY, A., TYSON, W. R. and COTTRELL, A. H., Phil. Mag., 15, 1967, 567.
16. WESTWOOD, A. R. C., PREECE, C. M. and KAMDAR, M. H., ASM Trans. Quart., 60, 1967, 723.
17. HAYDEN, H. W. and FLOREEN, S., Phil. Mag., 20, 1969, 135.
18. GILMAN, J. J., Trans. AIME, 212, 1958, 783.
19. STROH, A. H., Phil. Mag., 3, 1958, 597.
20. BULLOUGH, R., Phil. Mag., 9, 1964, 917.
21. KAMDAR, M. H. and WESTWOOD, A. R. C., Acta. Met., 16, 1968, 1335.
22. SMITH, E. and BARNBY, J. T., Metal Sci. Journ., 1, 1967, 56.
23. KAMDAR, M. H., Met. Trans., 2, 1971, 2937.
24. DERUYETTERE, A. and GREENOUGH, A. B., J. Inst. Met., 34, 1956, 337.
25. SHCHUKIN, E. D. and LIKHTMAN, V. I., Soviet Physics-Doklady, 4, 1959, 111.
26. KAMDAR, M. H., Met. Trans. 2, 1971, 485.
27. STROH, A. H., Adv. in Phys., 6, 1957, 418.
28. SMITH, E., Acta. Met., 14, 1966, 985.

Table 1 Occurrence of Embrittlement [1]

	Hg	Ga	Cd	Zn	Sn	Pb	Bi	Li	Na	Cs	In
Aluminum	x	x		x	x				x		x
Bismuth	x										
Cadmium		x			x					x	x
Copper	x						x	x	x		x
Iron	x	x	x	x		x		x			x
Magnesium				x					x		
Silver	x	x									
Tin	x	x									
Titanium	x		x								
Zinc	x	x			x						x

x denotes occurrence of embrittlement

Table 2 Values of Ratios of σ/τ for Some Typical Solid Metals Which are Embrittled by Liquid Metals [15]

Material	σ/τ	σ_{max}/τ_{max}
Cu	12.6	28.2
Ag	14.4	30.2
Au	24.7	33.8
Ni	7.9	22.1
Fe	8.5	6.75

Table 3 Summary of Test Data on Amalgamated Asymmetric Zinc Bicrystals, Kamdar and Westwood [8, 21]

Material	χ	τ_C (g/mm^2)	τ_F (g/mm^2)	ϕ_I in ergs/cm^2 via Equation (7)
Zinc	22°-75°	10 ± 3	35-95	45 ± 7
Zn-0.05 at % Cu	40° or 70°	61 ± 7	80-105	61 ± 5
Zn-0.2 at % Cu	16°-80°	95 ± 10	120-180	60 ± 7

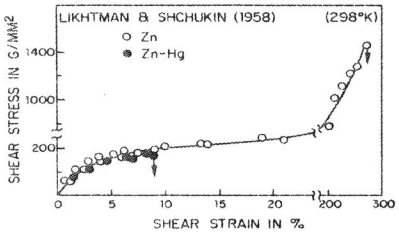

Figure 1 Stress-strain curves for (a) unamalgamated and (b) amalgamated zinc monocrystals at room temperature. $\chi_o = 48°$, after Likhtman and Shchukin [5].

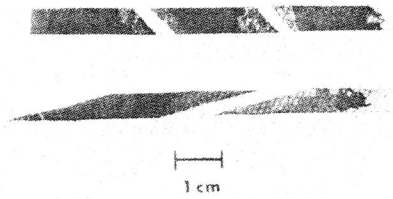

Figure 2 Demonstrating cleavage of cadmium monocrystals at 25°C following coating with mercury - 60 at pct indium solution, after Kamdar [1].

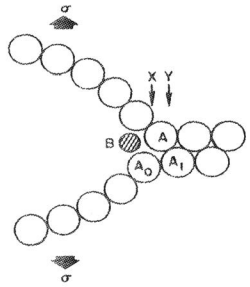

Figure 3 Illustrating (schematic) displacement of atoms at the tip of a crack. The bond A-A_o constitutes the crack tip and B is liquid metal atom.

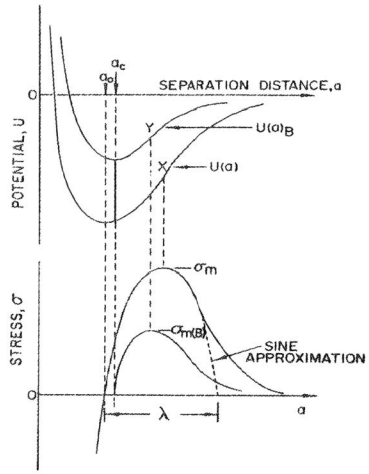

Figure 4 Schematic potential energy, U(a) and $U(a)_B$, and resulting stress, σ(a) and $\sigma(a)_B$, versus separation distance curves for bonds of type A-A_o (Figure 3) in the absence and presence of chemisorbed atom B. For spontaneous chemisorption of B, $a_c = a_o$. For strain-activated chemisorption, $a_c > a_o$, after Westwood and Kamdar [4].

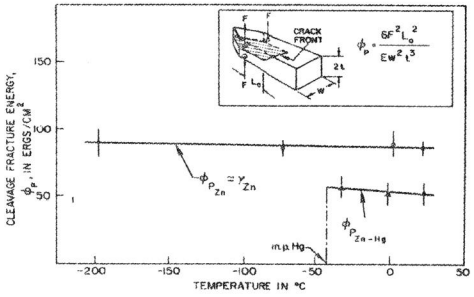

Figure 5 Effects of temperature and liquid mercury environment on the cleavage crack propagation energy, ϕ_p, for the (0001) planes of zinc. The inset shows the formula and type of specimens used to determine ϕ_p, after Westwood and Kamdar [4].

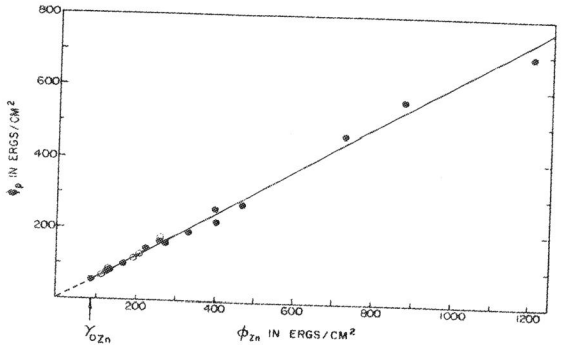

Figure 6 A comparison of the fracture energy involved in the propagation of a plastically blunted cleavage crack in air, $\phi_{p,Zn}$, and in mercury, $\phi_{p,Zn\text{-}Hg}$, from a double propagation experiment. A line of slope 0.61 is drawn through the data, after Westwood and Kamdar [4].

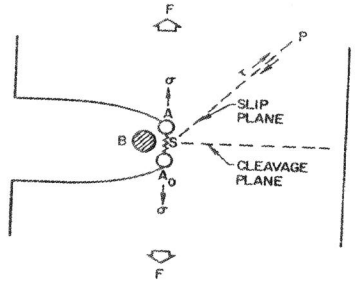

Figure 7 Schematic illustration of an "equilibrium" crack in a solid, subjected to an increasing force F. The bond A-A_0 constitutes the crack tip. B is a surface active liquid metal atom.

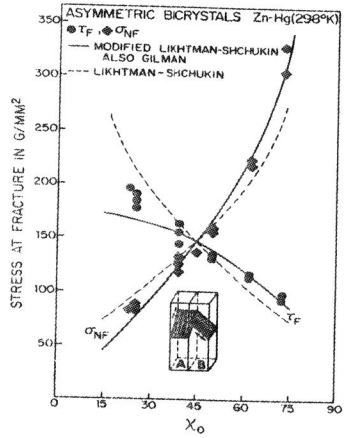

Figure 8 Orientation dependence of the normal stress, σ_{NF}, and shear stress, τ_F, at fracture for Type 1 asymmetric zinc bicrystals in the partially amalgamated condition. For comparison, the theoretically constructed curves correspond to solid lines -- Gilman or Kamdar-Westwood criteria [8], dashed lines -- after Likhtman-Shchukin [5].

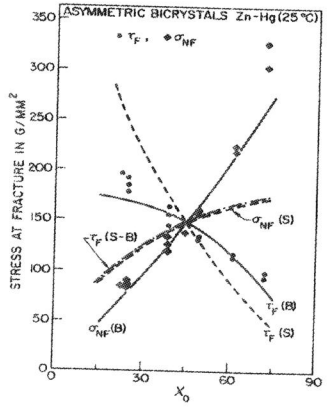

Figure 9 Some data as Figure 8. The solid lines, B, correspond to Bullough's [20] analysis; the dashed lines to Stroh's [19] analysis; and the other line, S-B, to Smith-Barnby's [22] analysis, after Kamdar and Westwood [8].

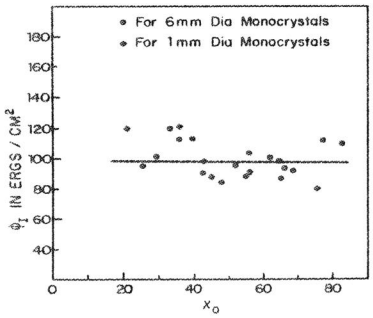

Figure 10 Illustrating the variation of the energy to initiate basal cracks in zinc monocrystals at 77°K with X_o and crystal diameter, after Kamdar [23].

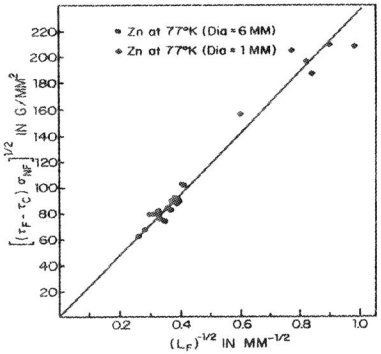

Figure 11 Illustrating linear relationship between the product $[(\tau_F-\tau_C)\sigma_{NF}]^{1/2}$ and $(L_F)^{-1/2}$ for zinc monocrystals of 1mm and 6mm dia. tested in tension at 77°K. The correlation shown is equivalent to Petch fracture-stress grain size relationship when L_F varied from 6.02 to 14mm, after Kamdar [23].

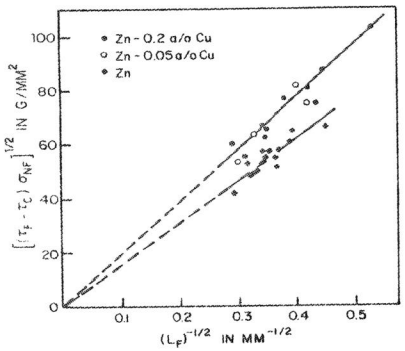

Figure 12 Illustrating linear relationship between the product $[(\tau_F-\tau_C)\sigma_{NF}]^{1/2}$ and $(L_F)^{-1/2}$ for partially amalgamated asymmetric bicrystals of zinc and it's alloys tested in tension at 298°K. The correlation shown is equivalent to the Petch fracture stress-grain size relationship, after Kamdar and Westwood [21].

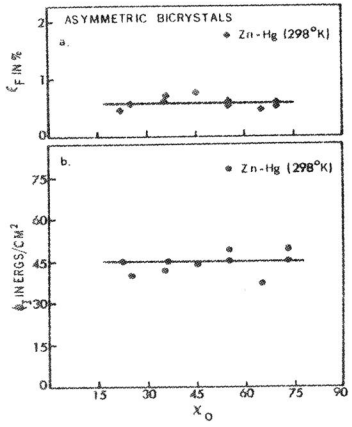

Figure 13 Orientation dependence of (i) the shear strain at fracture, ϵ_F, Figure 13(a) and (ii) the energy to initiate cleavage fracture on the basal plane, ϕ_I, for asymmetric bicrystals of zinc, Figure 13(b) in liquid mercury at 298°K, after Kamdar [1].